Pure Appl. Geophys.

DOI 10.1007/s00024-015-1162-2

Pure and Applied Geophysics

Integrated GPR and ERT as Enhanced Detection for Subsurface Historical Structures Inside Babylonian Houses Site, Uruk City, Southern Iraq

Emad H. Al-Khersan,[1] Jassim M. T. Al-Ani,[2] and Salah N. Abrahem[3]

Abstract—Uruk archaeological site, which located in Al-Muthanna Governorate southern Iraq, was investigated by integrated geophysical methods, ground penetration radar (GPR) and electric resistivity tomography (ERT) to image the historical buried structures. The GPR images show large radar attributes characterized by its continuous reflections having different widths. GPR attributes at shallower depth are mainly representing the upper part of Babylonian Houses that can often be found throughout the study area. In addition, radargrams characterized objects such as buried items, buried trenches and pits which were mainly concentrated near the surface. The ERT results show the presence of several anomalies at different depths generally having low resistivities. It is clear that the first upper zone can be found throughout the whole area and it may represent the top zone of the Babylonian houses. This zone is characterized by its dry clay and sandy soil containing surface broken bricks and slag mixed with core boulders. The second one underneath the top shows a prominent lower resistivity zone. It is probably caused by the moisture content that reduces the resistivity. The thickness of this zone is not equal at all parts of the site. The third deeper zone typically represents the archaeological walls. Most of the main anomalies perhaps referred to the buried clay brick walls. The map of the archaeological anomalies distribution and 3D view of the foundations at the study area using GPR and ERT techniques clearly show the characteristics of the Babylonian remains. A contour map and 3D view of Uruk show that the archaeological anomalies are concentrated mainly at the NE part of the district with higher values of wall height that range between 6 and 8 m and reach to more than 10 m. At the other directions, there are fewer walls with lower heights of 4–6 m and reach in some places the wall foot.

Key words: Uruk, Al-Muthanna, GPR and 2D-imaging, Babylon, remains, Emad Al-Khersan, Gilgamesh.

1. Introduction

Uruk represents Iraq's ancient site, which includes the vestiges of some of the world's earliest cities. It thrived from the beginning of the fifth millennium BC until the end of the third century AD, when it finally declined and was abandoned. Its ruins are covered by tens centimetres of sand (Pollock *et al.* 1996). Uruk is the first largest Sumerian settlements and the most important religious centres in Mesopotamia. The Sumerian traders have moved Uruk culture and surroundings. Uruk people gradually evolved their own economies comparing with other cultures (Beaulieu 2003). It is famous as the capital city of Gilgamesh, hero of the Epic of Gilgamesh. He built the city wall around Uruk and he was the king of it. Uruk citizens have designed very well canal system through the city that has been described as "Venicein the desert". This canal system flowed throughout the city connecting it with the maritime trade on the ancient Euphrates River as well as the surrounding agricultural belt (Fassbinder *et al.* 2003).

The studied archaeological site of this research is located between the longitudes 45°37′28″E–45°39′7.3″E and latitudes 31°18′34.5″N–31°20′14.5″N. It is situated about 30 km east of Al-Muthanna Governorate, southern Iraq near the boundary between the Mesopotamia and the southern desert. Moreover, Hritz (2012) had been drawn subsoils column at the marshes region nearby the Uruk site (Fig. 1). The maximum extent of this site is 3 km N–S and 2.5 km E–W covering an area of about 5.5 km^2. It lies within the lower parts of Mesopotamia that is characterized by its flat topography (Buday 1980). Hills of ancient civilization inside the investigated site represent the historical buildings such as, houses and temples or

[1] Geology Department, College of Science, Basrah University, Basrah, Iraq. E-mail: emreal60@yahoo.com
[2] Geology Department, College of Science, University of Baghdad, Baghdad, Iraq. E-mail: jassimthabit@yahoo.com
[3] Physics Department, College of Science, University of Al-Muthanna, Al-Muthana, Iraq. E-mail: zircon200036@yahoo.com

Published online: 14 August 2015

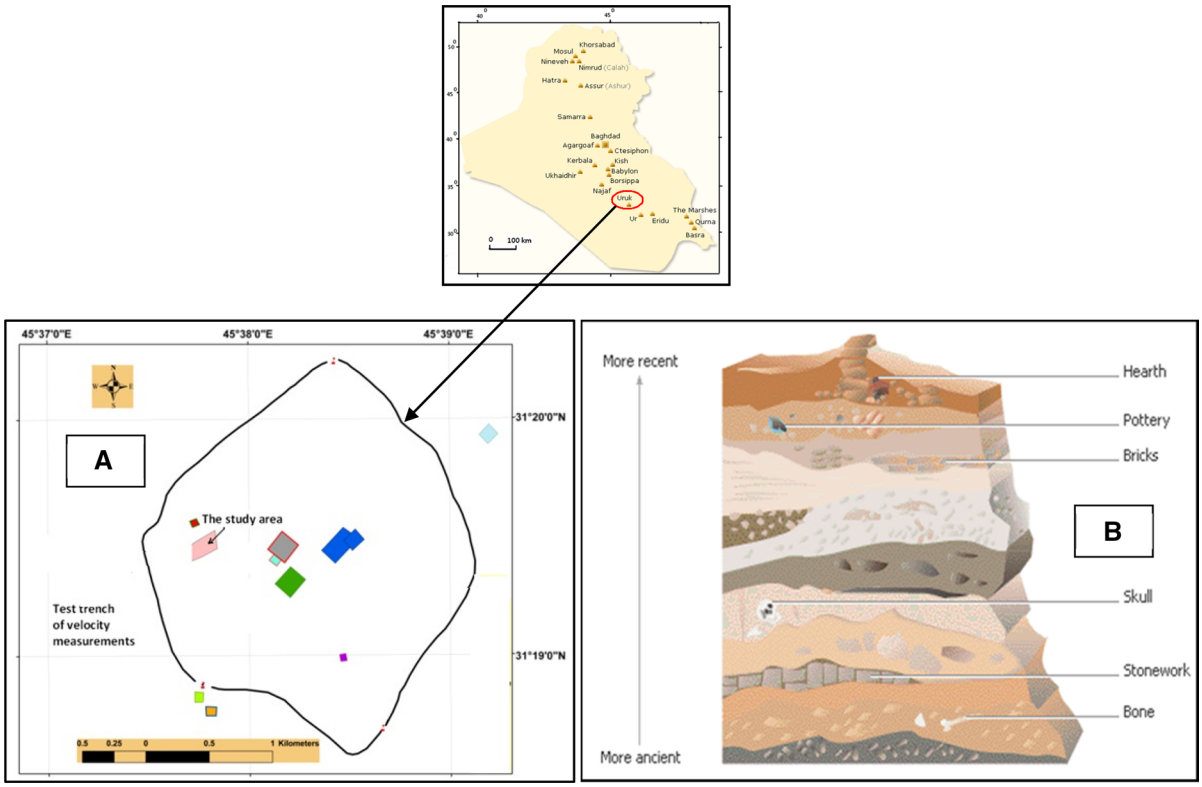

Figure 1
a Location map of the study area (Babylon Houses); and **b** subsoil column inside URUK site (Hritz 2012)

ziggurats (Baker 2002). The study area was covered by the Quaternary alluvium deposits. It mainly consists of clay, silt and sand sediments (Al-Hashimi 1974). Different materials such as bricks, debris, sediment from channels, undisturbed soil and sun-baked bricks are scattered on the ground surface of the area. There are many exposed buildings such as walls, temples, arced gates and tombs. Most of the exposed walls have widths ranging from approximately 1–2 m. The dimensions and design of clay bricks are different. The important point for geophysical surveying, some 5000 years later, is the fact that Gilgamesh used baked (burnt) bricks for the walls he built. The enrichment of ferromagnetic minerals such as Magnetite in the archaeological structures is owing to the use of fire and magneto tactic bacteria in organic debris (Fassbinder and Becker 2001). The early wall of Uruk had a mantle of baked bricks, filled with cheaper mud bricks, which would give an ideal base for electrical prospecting because of the conductivity of burnt clay. Since any drilling in the archaeological sites is not allowed, the data about the groundwater are obtained from an artesian well located at a close village with coordinates of 45°15′E and 31°26′N about 500 m west of the study area. The well is drilled by the General Commission for Groundwater (GCGW)/Al-Muthanna branch. The static water level in this well is 3 m from the natural ground surface; moreover, the mobile water depth is at 4.7 m. The electrical conductivity of groundwater sample is measured and found to be 2000 microMohs/cm (high salinity media).

The main objectives of this study are:

1. Comparison between the common electrical arrays of the ERT technique to find the most suitable array for the study area that leading to the best results.

2. Using GPR and ERT techniques to determine the positions and depths of underneath archaeological remains inside Uruk site. Therefore, a map for the buried remains can be deduced.
3. Comparison between both GPR and ERT surveys in delineating the accurate depth and shape of the subsurface.

2. Field Work

To define an accurate coordinate information for the study area, we made use of Garmin GPS, total station, and Arc GIS 9.3. The result of this step produced a topographic map to the area (Fig. 2). The locations of GPR and ERT profiles were determined according to this map as grids of GPR and ERT surface lines.

2.1. GPR Data Acquisition

We have used Sweden MALA Geosciences RAMAC/GPR field equipment of mono-static 250 MHz ground-coupled shielded antenna. Before starting the data production, we considered equipment capability to resolve the target archaeological feature. Thus, we performed a man-made testing facility. The followed steps are described below:

- A location was selected outside the western gate of Uruk city in contact with the city wall of the archaeological site, and a trench was dug at this location with dimensions of 1.75 × 1.1 m and depth 1.8 m.
- Different archaeological materials such as bricks, debris, sediments from channels, undisturbed soil and sun-baked bricks scattered here and there in settlement, are collected, buried and are covered by

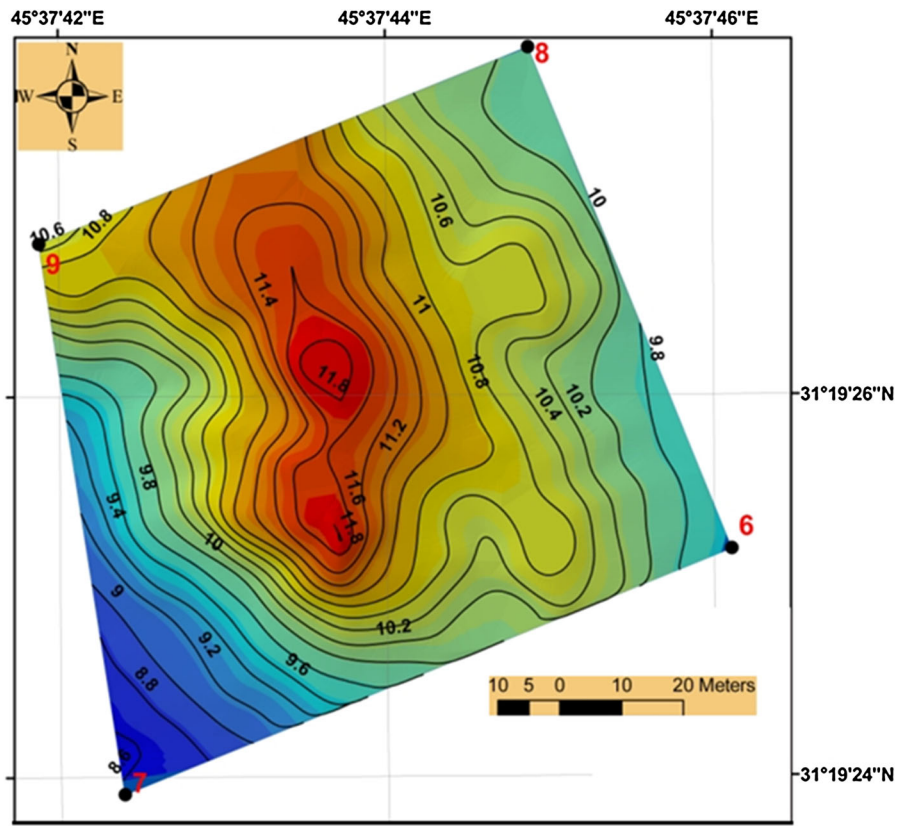

Figure 2
The topographic map of the Babylonian houses and the surroundings

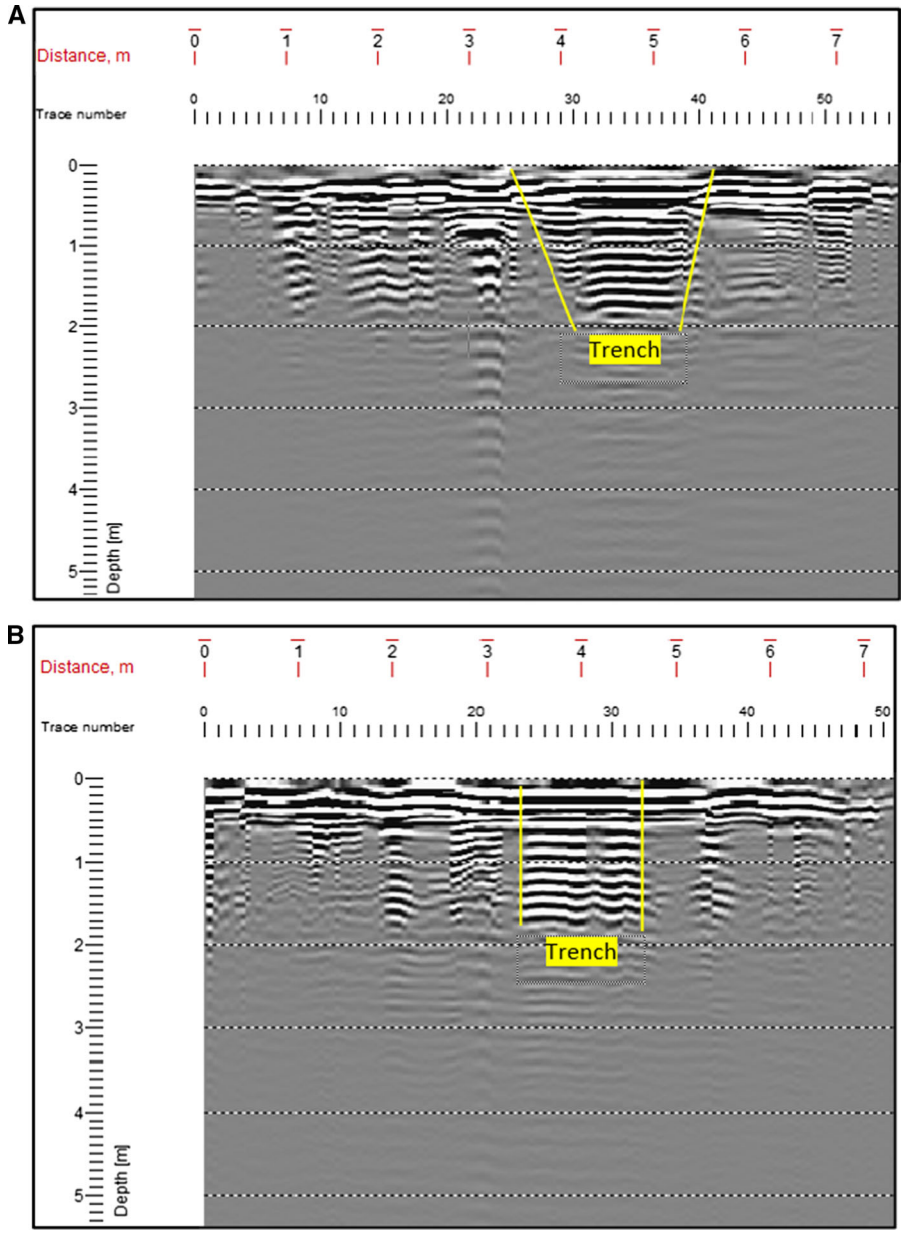

Figure 3
GPR tested profiles **a** *above* and **b** *below*

thin veneer of soil. These materials were returned back to their original positions after GPR test.

- Several GPR settings were used until the suitable one is chosen and then applied for all selected profiles. These settings are: number of trace stack is 4 and sometimes autostack, antenna spacing from ground surface is 0.1 m, sampling interval 0.4 m, time window 203 ns, sampling frequency 2607 MHz and time sampling interval is 0.7 ns. Therefore, two perpendicular GPR profiles were conducted over this artificial buried wall, the first profile (A) trends SE–NW, and the other (B) trends NE–SW (Fig. 3).
- The two-way travel times from the radargrams were measured; and then the depth of the artificial wall is known, the velocity is measured using the

travel time from the GPR record and the known reflector depth (d). The average velocity (v) of the radar signal can be determined from the formula: (Oswin 2009)

$$V = \frac{2d}{t} \qquad \therefore V = \frac{2d}{t} = \frac{2 \times 1.8}{36} = 0.1\,\mathrm{m/ns}$$

t, total time and the antenna is directly over the known target.

Therefore, the average velocity of 0.10 m/ns is applied for all sections on the basis of known depth to reflector. The topographic variation inside the studied area was surveyed precisely, so that the GPR profiles can display with correct topography. A grid pattern parallel GPR survey system was carried out in the area and ninety SW–NE parallel profiles with 1 m spacing between each other were conducted in October 2011.

2.2. *ERT Data Acquisition*

Before starting the data production, we considered the best-fit electrode configuration tests to resolve the target archaeological feature. In other words, we tested the best suitable spreading geometry at the site. This step is represented by deploying different electrode configurations at the same profile location. We compared the results of three common electrical resistivity configurations (i.e. Wenner, Wenner–Schlumberger and dipole–dipole). The comparison focused on the resolution efficiency at the site (Loke 2010). To investigate the imaging capabilities of these electrode configurations, three test survey profiles, which are URUK-TEST-WEN, URUK-TEST-WEN-SCH and URUK-TEST-DIPDIP corresponding to Wenner, Wenner–Schlumberger and dipole–dipole configurations, were carried out using the Sweden ABEM Terrameter SAS-4000 Lund imaging multi-electrode system. The electrode layout of these profiles is ranged from 0 to 60 m and the electrode basic spacing is 1.5 m. It is known that each of the electrode arrays has its own advantages and limitations in fieldwork. The image created by means of the ERT for the same structure will be different for each array. For these reasons, choosing the right one for the resistivity surveys is important (Loke 2010). For resistivity imaging, the electrode arrays might have different imaging abilities for a model, i.e. differences in spatial resolution, tendency for artefacts in the images, deviation from the true model resistivity and interpretable maximum depth. The sensitivity patterns play important roles for the resolving capability in the inversion of the data. To obtain a high resolution and reliable image, the electrode array used should ideally give data with the maximum anomaly information and reasonable data coverage.

The choice of the best array for a field survey depends on the type of structure to be mapped, the sensitivity of the resistivity metre and the background noise level. Among the characteristics of an array that should be considered are (1) sensitivity of the array to vertical and lateral changes in the subsurface resistivity, (2) depth of investigation, (3) horizontal data coverage (4) signal strength (Loke 2004) (5) resolution for the different models (6) imaging quality with different data densities and (7) sensitivity to noise levels (Dahlin and Zhou 2004). The first two characteristics can be determined from the sensitivity function of the array for a homogeneous earth model. The sensitivity function basically tells us the degree to which a change in the resistivity of a section of the subsurface will influence the potential measured by the array. The higher the value of the sensitivity function is the greater of the influence of the subsurface region on the measurement. Here, we try to discuss some of them as follows:

2.2.1 *Sensitivity of the Array to Vertical and Horizontal Changes*

For the Wenner array, the sensitivity sections (Fig. 4) show large values near the surface between C1 and P1 electrodes, as well as between C2 and P2 electrodes. This means that if a small body with a higher resistivity than the background medium is placed in these zones, the measured apparent resistivity value will decrease. This phenomenon is also known as an “anomaly inversion”. In comparison, if the high resistivity body is placed between the P1 and P2 electrodes where there are large sensitivity values, the measured apparent resistivity will increase. This is the basis of the offset Wenner method by Barker

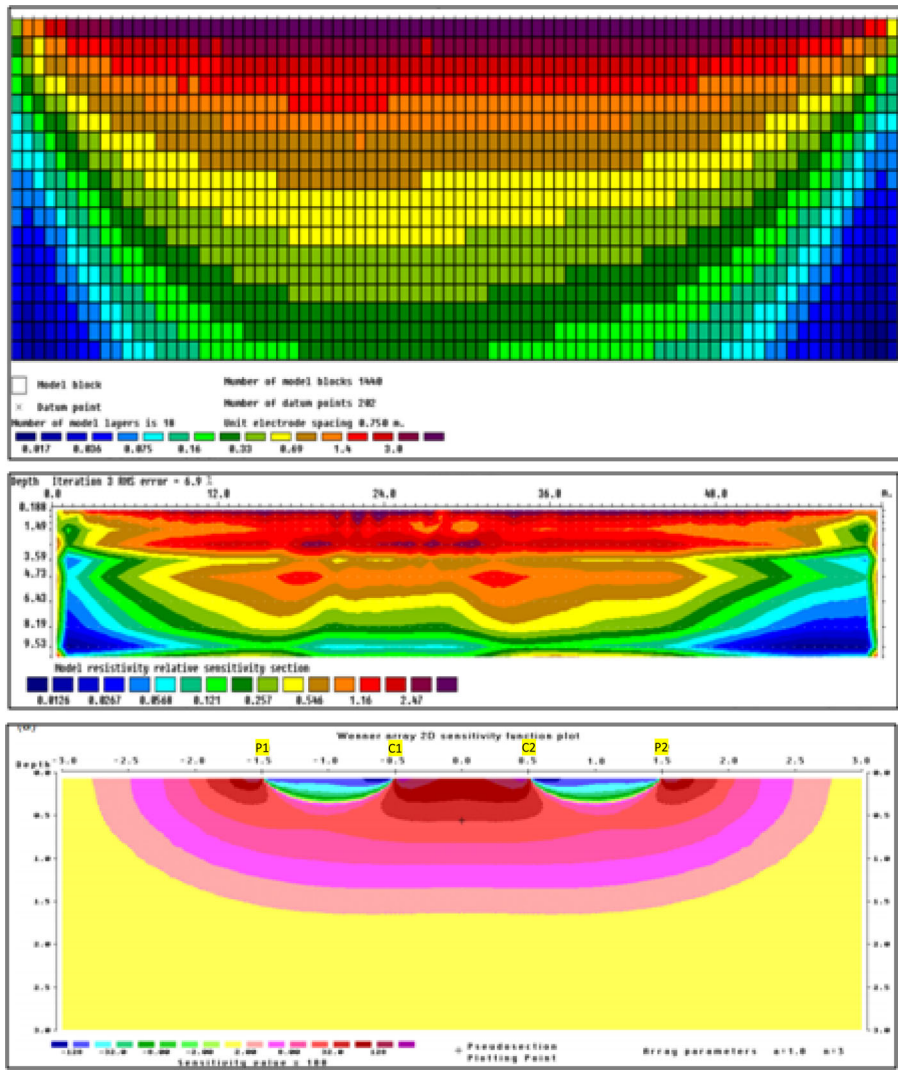

Figure 4
The subsurface sensitivity (*above*), the blocks sensitivity (*middle*) and the sensitivity (*below*) sections of the test survey Profile URUK-TEST-WEN for Wenner array

(1992) to reduce the effects of lateral variations in resistivity sounding surveys. In these sections, the sensitivity plot for the Wenner array has almost horizontal contours beneath the centre of the array. Because of this property, the Wenner array is relatively sensitive to vertical changes in the resistivity below the centre of the array. However, it is less sensitive to the horizontal changes. In general, Wenner array is good in resolving vertical changes (i.e. horizontal structures), but relatively poor in detecting horizontal changes (i.e. narrow vertical structures).

Figure 5 shows the sensitivity sections for the Wenner–Schlumberger array. The sensitivity contours of this array have a slight vertical curvature below the centre of the array. At high "*n*" values, the high sensitivity lobe beneath P1 and P2 electrodes becomes more separated from the high sensitivity values near C1 and C2 electrodes. This means that this array is moderately sensitive to both horizontal (for low "*n*" values) and vertical structures (for high "*n*" values).

Dipole–dipole array has been, and is still, widely used in resistivity because of the low EM coupling

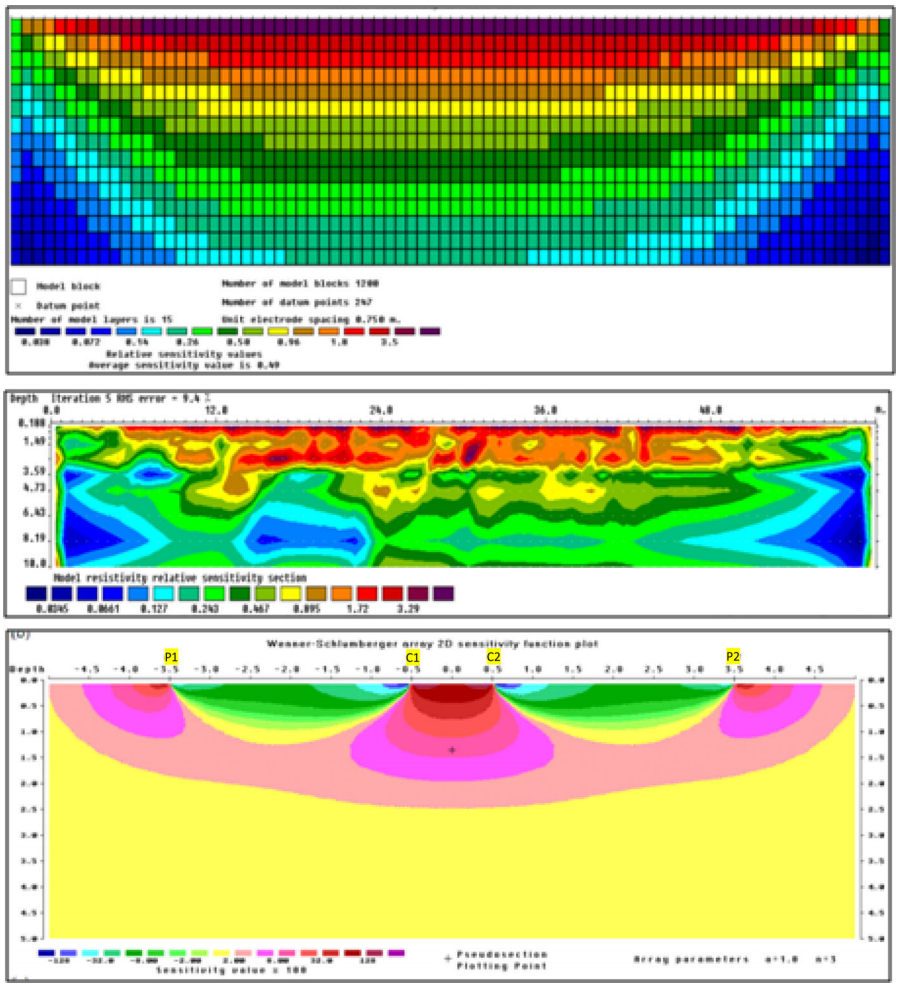

Figure 5
The subsurface sensitivity (*above*), the blocks sensitivity (*middle*) and the sensitivity (*below*) sections of the test survey Profile URUK-TEST-WEN-SCH for Wenner–Schlumberger array

between the current and potential circuits. The sensitivity contour pattern becomes almost vertical for "*n*" values greater than 2. Thus, the dipole–dipole array is very sensitive to horizontal changes in resistivity, but relatively insensitive to vertical changes in the resistivity. That means it is good in mapping vertical structures, such as walls, archaeological groove and cavities, but relatively poor in mapping horizontal structures (Fig. 6).

2.2.2 *The Inverse Model and Depth Investigation*

Another three tests on the same profile were conducted to examine the imaging capabilities of these arrays for the inversion models (Fig. 7). The depth of investigation of the Wenner, Wenner–Schlumberger and dipole–dipole arrays at this test survey is equal to 11, 8.68 and 6.13 m, respectively. A median depth of investigation means that the upper section of the earth above the "median depth of investigation" has the same influence on the measured potential as the lower section. This tells us roughly what depth we can see with an array. This depth does not depend on the measured apparent resistivity or the resistivity of the homogeneous earth model. It should be noted that the depths are strictly only valid for a homogeneous earth model, but they are probably good enough for planning field surveys.

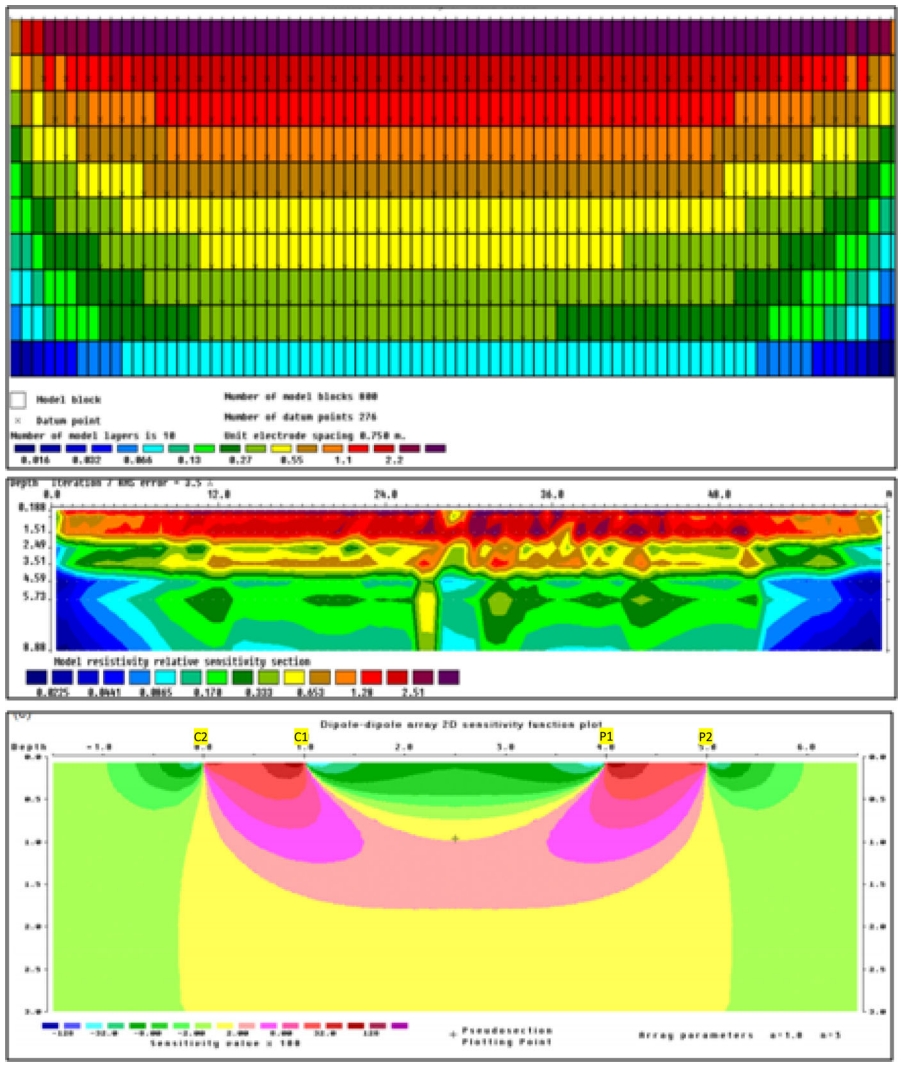

Figure 6
Shows the subsurface sensitivity (*above*), the blocks sensitivity (*middle*) and the sensitivity (*below*) sections of the test survey Profile URUK-TEST-DIPDIP for dipole–dipole array

If there are large resistivity contrasts near the surface, the actual depth of investigation could be somewhat different. In general, the dipole–dipole array has a shallower depth of investigation compared to the Wenner and Wenner–Schlumberger arrays for ERT survey.

From these models, one can see that the dipole–dipole array measurement yields the highest resolution and the best image for vertical anomalies. The Wenner and Wenner–Schlumberger arrays have similar behaviour of imaging ability due to the resemblance of their electric field and measurements,

Figure 7 ▶
The measured and the inverse model of the test survey Profile URUK-TEST-WEN for Wenner, Wenner–Schlumberger and dipole–dipole configurations

with their main strength in the depth determination, which is good in relation to the dipole–dipole array. However, the spatial resolution of the Wenner array is poorer than the dipole–dipole and Wenner–Schlumberger arrays. The imaging resolution of the dipole–dipole is better than others, particularly for the location of vertical structures. Accordingly, the

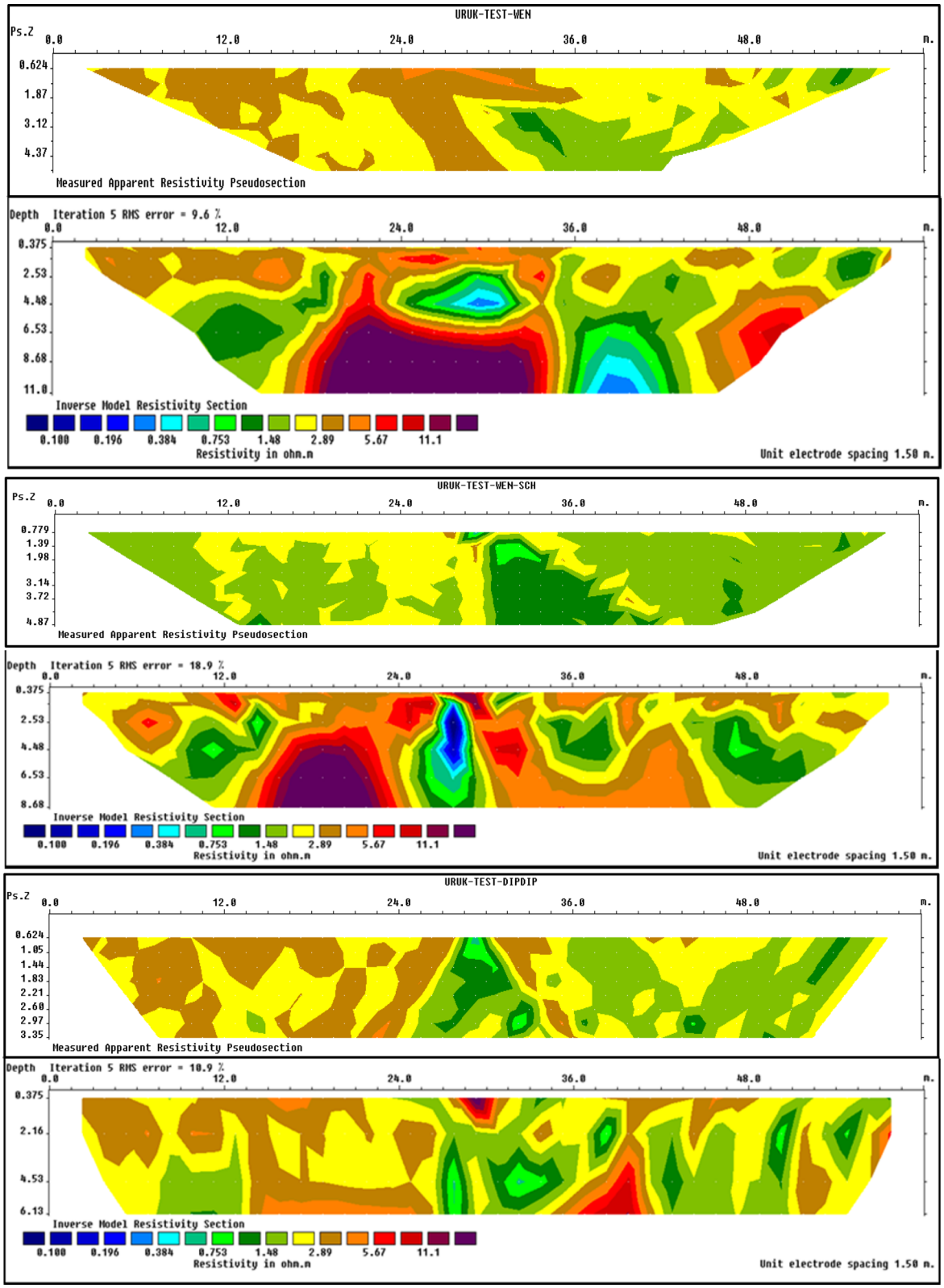
URUK-TEST-WEN
Ps.Z
0.0
12.0
24.0
36.0
48.0
m.
0.624
1.87
3.12
4.37
Measured Apparent Resistivity Pseudosection
Depth
Iteration 5 RMS error = 9.6 %
0.375
2.53
4.48
6.53
8.68
11.0
Inverse Model Resistivity Section
0.100
0.196
0.384
0.753
1.48
2.89
5.67
11.1
Resistivity in ohm.m
Unit electrode spacing 1.50 m.
URUK-TEST-WEN-SCH
Ps.Z
0.779
1.39
1.98
3.14
3.72
4.87
Measured Apparent Resistivity Pseudosection
Depth
Iteration 5 RMS error = 18.9 %
0.375
2.53
4.48
6.53
8.68
Inverse Model Resistivity Section
0.100
0.196
0.384
0.753
1.48
2.89
5.67
11.1
Resistivity in ohm.m
Unit electrode spacing 1.50 m.
URUK-TEST-DIPDIP
Ps.Z
0.624
1.05
1.44
1.83
2.21
2.60
2.97
3.35
Measured Apparent Resistivity Pseudosection
Depth
Iteration 5 RMS error = 10.9 %
0.375
2.16
4.53
6.13
Inverse Model Resistivity Section
0.100
0.196
0.384
0.753
1.48
2.89
5.67
11.1
Resistivity in ohm.m
Unit electrode spacing 1.50 m.

Table 1

The densities of data points of the three test survey profiles

Configuration	Density of data points
Wenner	202
Wenner–Schlumberger	247
Dipole–dipole	276

dipole–dipole array was chosen for future ERT surveys within the study area.

Finally, to obtain a high resolution and reliable image, the electrode array used should ideally give data with maximum anomaly information and reasonable data coverage (AIZEBEOKHAI 2010). Consequently, resistivity acquisition included a 32 parallel ERT northeast profiles each being 100 m long, comprising 41 electrodes were collected in February, 2012 over an area of 9300 m^2, with 2.5 m electrode spacing using the suitable dipole–dipole array. The spacing between these profiles equals 3 m to give systematic information about the area understudy.

2.2.3 Horizontal Data Coverage

One disadvantage of the Wenner array for 2D-resistivity imaging surveys is the relatively poor horizontal coverage as the electrode spacing is increased and the dipole–dipole array has better horizontal data coverage than the Wenner. The horizontal data coverage for Wenner–Schlumberger array is slightly wider than the Wenner array, but narrower than that obtained with the dipole–dipole array. Table 1 illustrates that the data points of the dipole–dipole survey are more than the other surveys. This means that the survey time for the dipole–dipole array is longer than the others.

3. Results and Discussion

3.1. GPR Interpretation

The greater the amplitude of wave reflections through a medium is, the greater the difference in chemical and physical characteristics of the buried material. The change in contrast on the GPR profile is isolated regions of high and/or low contrast. Amplitude may be analysed to understand the possible material compositions of buried targets. It is important to note that the unique reflections created by covered features may change from site to site based on geological factors such as soil saturation levels or complications attributed to ground coupling. However, with the knowledge of what to look for, data interpretation, while not easy, will in time become much less confusing. Although there is some consistency in the identification of the major target types, there is rarely a way to identify exactly what material the target is made of. Hypothetically, the compact sediments may not display a visual change upon excavation, but the GPR may give a change in amplitude in the region, due to the physical change (resistivity) in relation to the surrounding earth. Waveforms often signify the boundaries of subsurface changes. It is made of wavelets, which is a positive or negative shift in amplitude. These are formed as a result of the change in physical or chemical property of the targets that the signal encounters, and they often signify the top and bottom of buried items. When combined, the wavelets create a waveform, which is then compiled with the other waveforms from any given GPR sample to create a composite amplitude trace, or image of what lies beneath the GPR unit. Among many other uses, the analysis of these waveforms allows to understand subsurface of the survey region. Areas of low-amplitude waves usually indicate uniform matrix material or soils while those of high amplitude denote areas of high subsurface contrast such as buried archaeological features, voids or important changes. Lateral changes in amplitude, phase or reflection patterns in the radar record can be caused by changes in rock, soil type and moisture content.

RadExplorer, Ver.1.4-GX software (2005) was used to process and interpret the collected GPR data. The GPR raw data processing includes Dc removal, background removal, bandpass filter and predictive deconvolution. Time adjustment and topography have been applied for all the profiles in this study and processed with the same range of filter values, because the study area contains subsurface targets with the same original lithological characters (clay and silt). The presence of clay layer has an influence which causes high adsorption of the electromagnetic

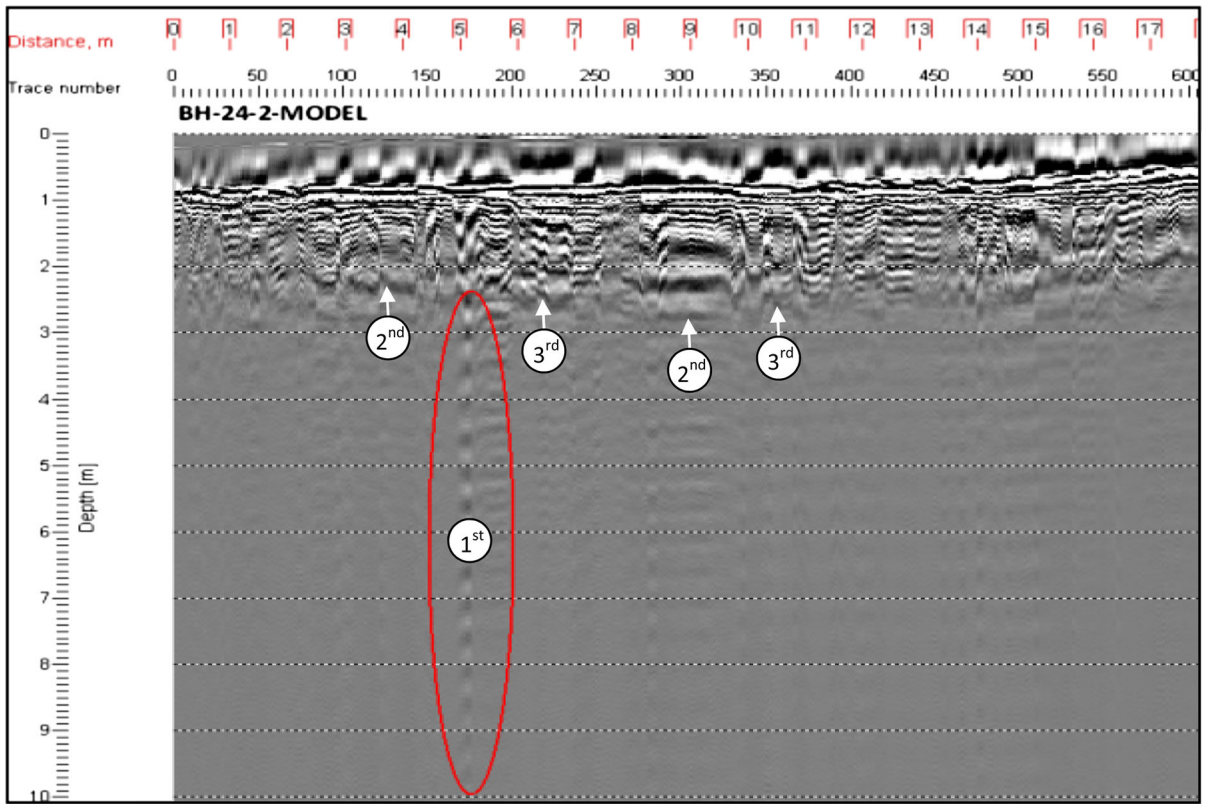

Figure 8
GPR model of profile (BH-24-2-MODEL) shows dense or reflective (1st) sub-horizontal buried items

energy that limits its penetration to not deeper than 2–3 m, although dielectric permittivity of the dried subsoil may have low value due to water table that exceeds nearly 5 m below surface. For this reason, the GPR data show maximum depth not more than 5 m. According to the above facts and results, and from reviewing the models of the Babylonian houses district, it is clear that:

- The first type of the image features is present with shallow depth of attributes with sub-horizontal, partly wavy reflections; however, it can often be found throughout the whole area representing the top part of the Babylonian houses district. This zone is characterized by dried clay and sandy soil including broken and weathered different archaeological materials such as broken brick and slag mixed with core boulders. These processes produce shallow layers of clay and sand deposits with different archaeological materials such as broken brick and slag.
- The second type of reflections shows deep attributes. These are characterized by continuous reflections with different widths. These reflections are typical feature for the archaeological walls. Most of the main attributes perhaps refer to buried remains of clay brick walls. The archaeological walls have approximated real depth between 1 and 6 m, and width from 1 to 2 m.
- The third type of reflections represents the point reflection attributes (small hyperbola) which are presented at the upper and/or the lower parts of the images. They occur either within the first or second type of reflections. The third type of reflections includes four subtypes of reflections, these are:
  - The 1st subtype is dense or reflective buried items, which are capable of creating echoes. The GPR signals cannot penetrate these objects. This phenomenon creates high-amplitude signals of repeating or echoing bands upon the screen. The electromagnetic wave bounces back and forth

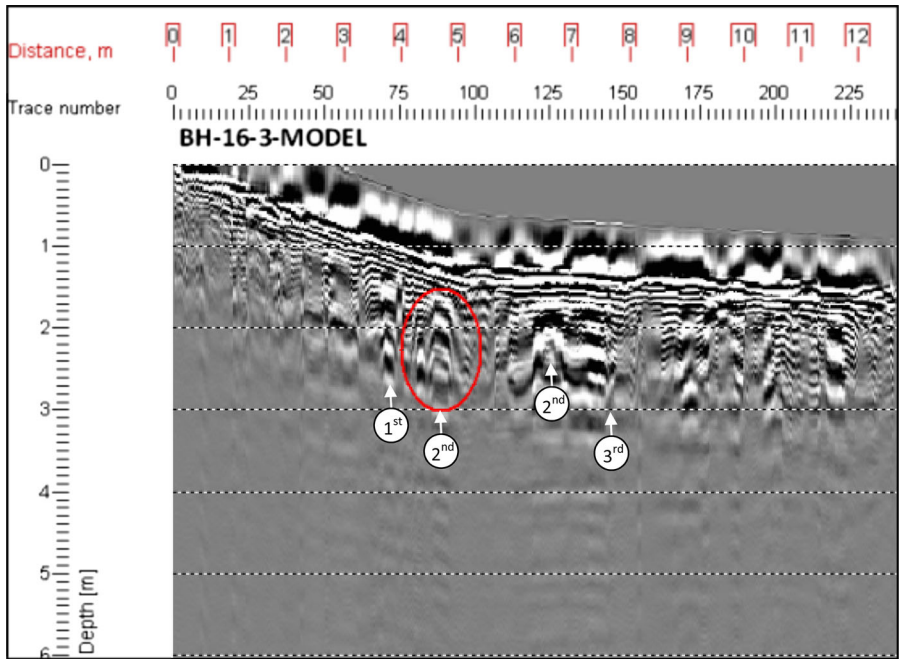

Figure 9
GPR model of profile (BH-16-3-MODEL) shows parabola (2nd) represented an object which is located at apex of an arc

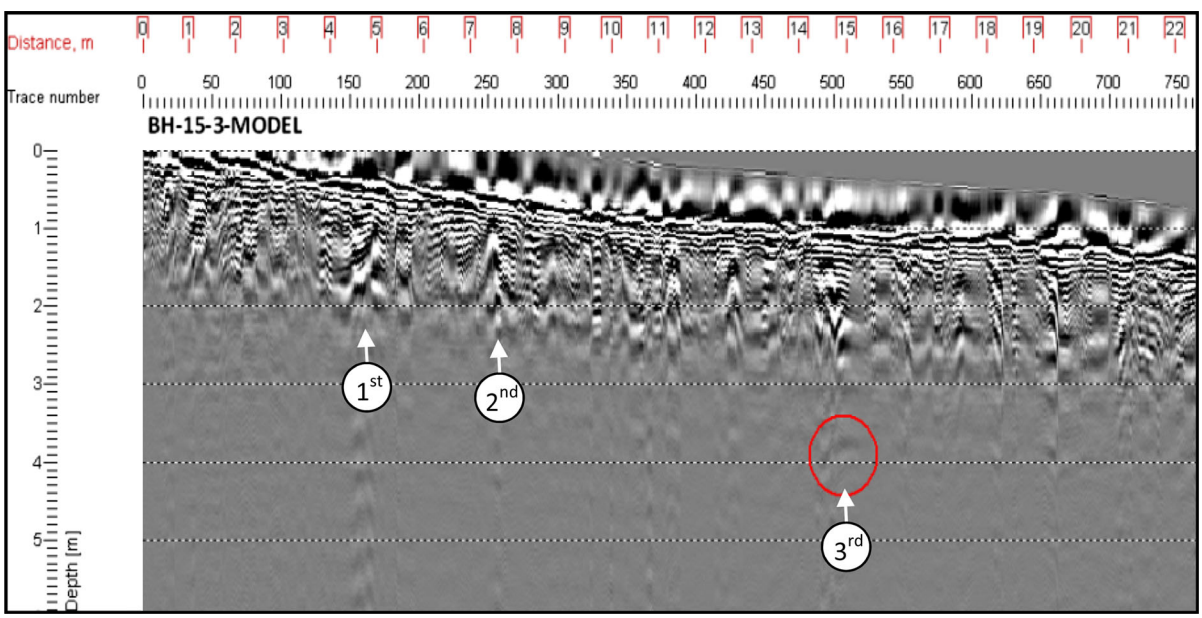

Figure 10
GPR model of profile (BH-15-3-MODEL) shows planar reflection (3rd)

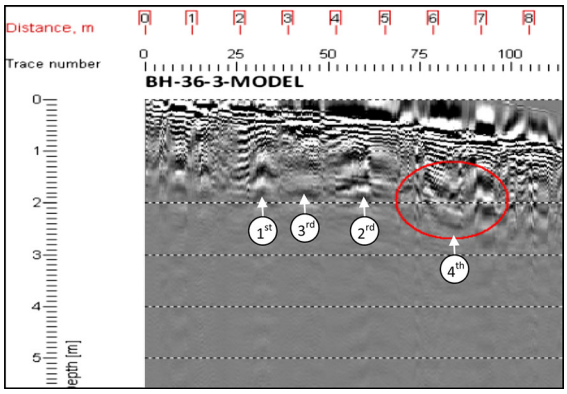

Figure 11
GPR model of profile (BH-36-3-MODEL) shows buried trenches and pits create cup-shaped (4th)

from the highly reflective object to the GPR device over and over again. The reflected signature from the dense or reflective buried item is at most times unmistakable. The buried features are capable of creating parabolic signatures such as coffins, ceramics, bricks or boulders (Fig. 8).

– The 2nd subtype is a parabola which represents an object located at the apex of the arc. Small hyperbola is created as the GPR footprint moves across rounded object. Reflections of this type are distinct and relatively easy to identify (Fig. 9).
– The 3rd subtype is the planar reflections. These reflections are occurring from buried targets and take the form of planar reflections. They appear as horizontal attributes and exhibit higher amplitude in relation to the surrounding matrix. These reflections are often the result of a physical discontinuity or a horizontal feature of archaeological interest. They may identify the layering of the soil. In general, it gives regular reflections along the GPR profile with some distinguished features here and there may refer to the small archaeological remains (Fig. 10).
– The 4th subtype is presented as buried trenches and pits. Covered pits and V-shaped trenches are identifiable features. The signatures indicate pit-like features and trenches. This creates high-amplitude cup-shaped or V-shaped signature on the display screen (Fig. 11). Covered pits may indicate the presence of grave pits.

Figure 12 is an example of the interpreted three segments of the GPR profile lines of Babylonian houses district showing the mentioned different types of radargram attributes at the study area.

3.2. *ERT Interpretation*

Also, the RES2DINV software is used to interpret the measured raw apparent resistivity data. This software uses the rapid least-squares inversion method to model the final resistivity sections. The optimization method basically tries to reduce the difference between the calculated and measured apparent resistivity values by adjusting the resistivity of the model blocks. A measure of this difference is given by the root-mean-squared (RMS) error. However, the model with the lowest possible RMS error can sometimes show large and unrealistic variations in the model resistivity values and might not always be the best model from a geological perspective. In general, the most prudent approach is to choose the model at the iteration after which the RMS error does not change significantly. This usually occurs between 3rd and 5th iterations (Loke and Dahlin 2002).

Figure 13 displays the ERT model of profiles 12, 15 and 32 as examples of the inverse model in the study area. The 2D resistivity imaging profiles have maximum depth of investigation of 13.5 m. A comparison of the results from adjacent profiles shows almost similar anomalies at similar depths. The resistivity of subsurface material is affected by porosity (shape, size and connection of pores), moisture (water) content, dissolved electrolytes, temperature of pore water, conductivity of minerals, the chemistry of the groundwater and other fluids trapped in the pore spaces within the soil matrix and/or the presence or absence of buried debris and structures. For a typical site, fine materials such as clay and silt are generally less resistive while coarse sand and gravel are generally more resistive. The soil (clay or sand) will appear more resistive when it is dry and less resistive when it is wet. The presence of subsurface walls often appears as a vertically oriented anomaly, and may be either conductive or resistive

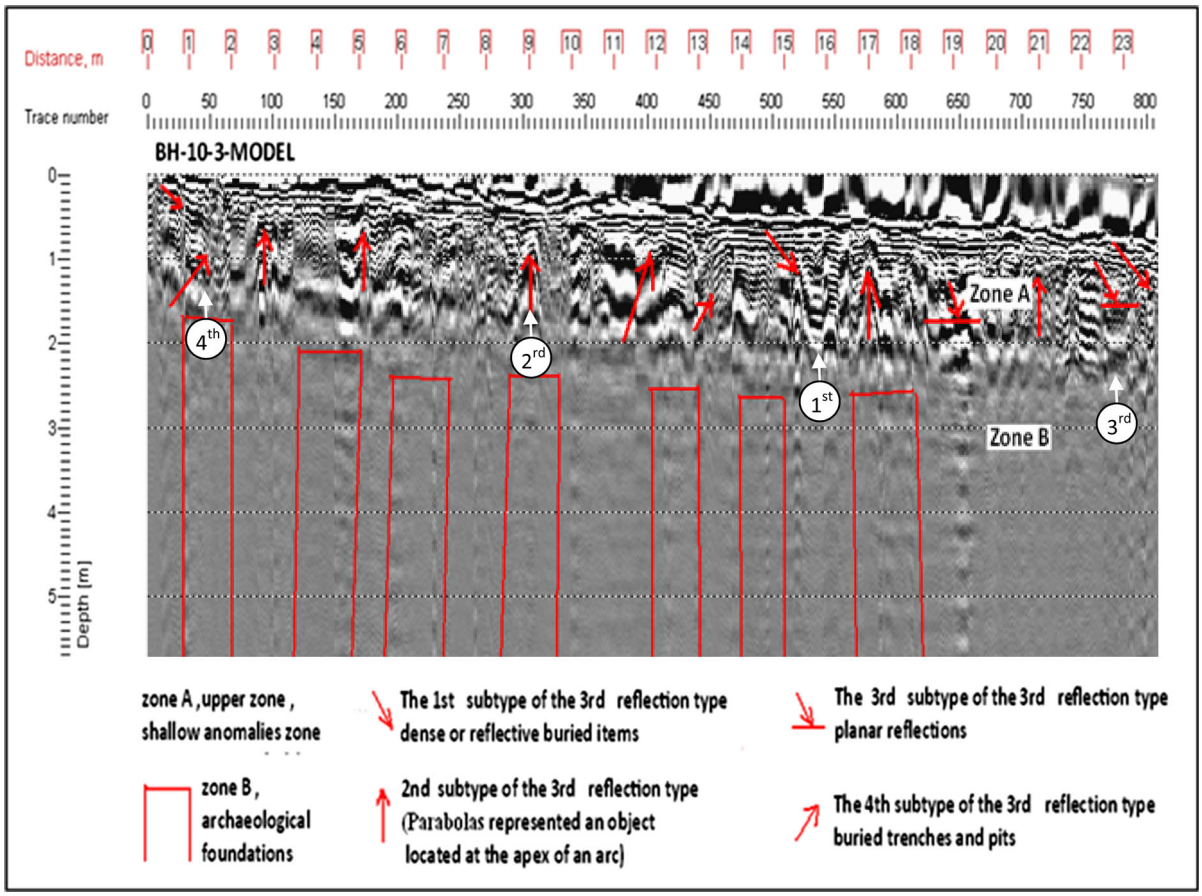

Figure 12
Interpreted example of three segments of (BH-10-3-.MODEL) GPR profile showing the legend of the different types of radargram attributes at the study area

depending on what type of fluid present (e.g. clean groundwater and/or unweathered/weathered contamination). Resistivity is linked to moisture content or porosity. Features such as wall foundations will give a relatively high resistivity response, while ditches and pits that retain moisture give a lower one. The archaeological graves can be considered as a lateral anomaly in a homogenous medium similar to the tunnel and cavity. An anomalous zone of the water- or clay-filled archaeological grave is distinguishably as very low or lowest resistivity zone, surrounding with the higher background. High resistivity zones are correlated with air-filled archaeological structures such as graves, caves, voids or holes in the overburden that had formed over archaeological walls. In general, in the archaeological structures, competent structures have high resistivity. Weathered rocks would show a much lower resistivity than the competent one. High-conductivity zone in the resistivity images may be due to infilling by clay, or water within the pores. Generally, all the resistivity values are very low to low values not exceeding more than 11.1 Ohm m due to corresponding site subsoils or layers: The interpretation of all models basically declares the presence of three zones underneath Uruk site as mentioned below:

The upper one with a resistivity value (2.89–5.67 Ohm m) is interpreted as an alluvium soil consisting of sand and clay. In Uruk, weathering of archaeological structures produces clayed and sandy soil with core boulders and other partially weathered material because these structures are constructed

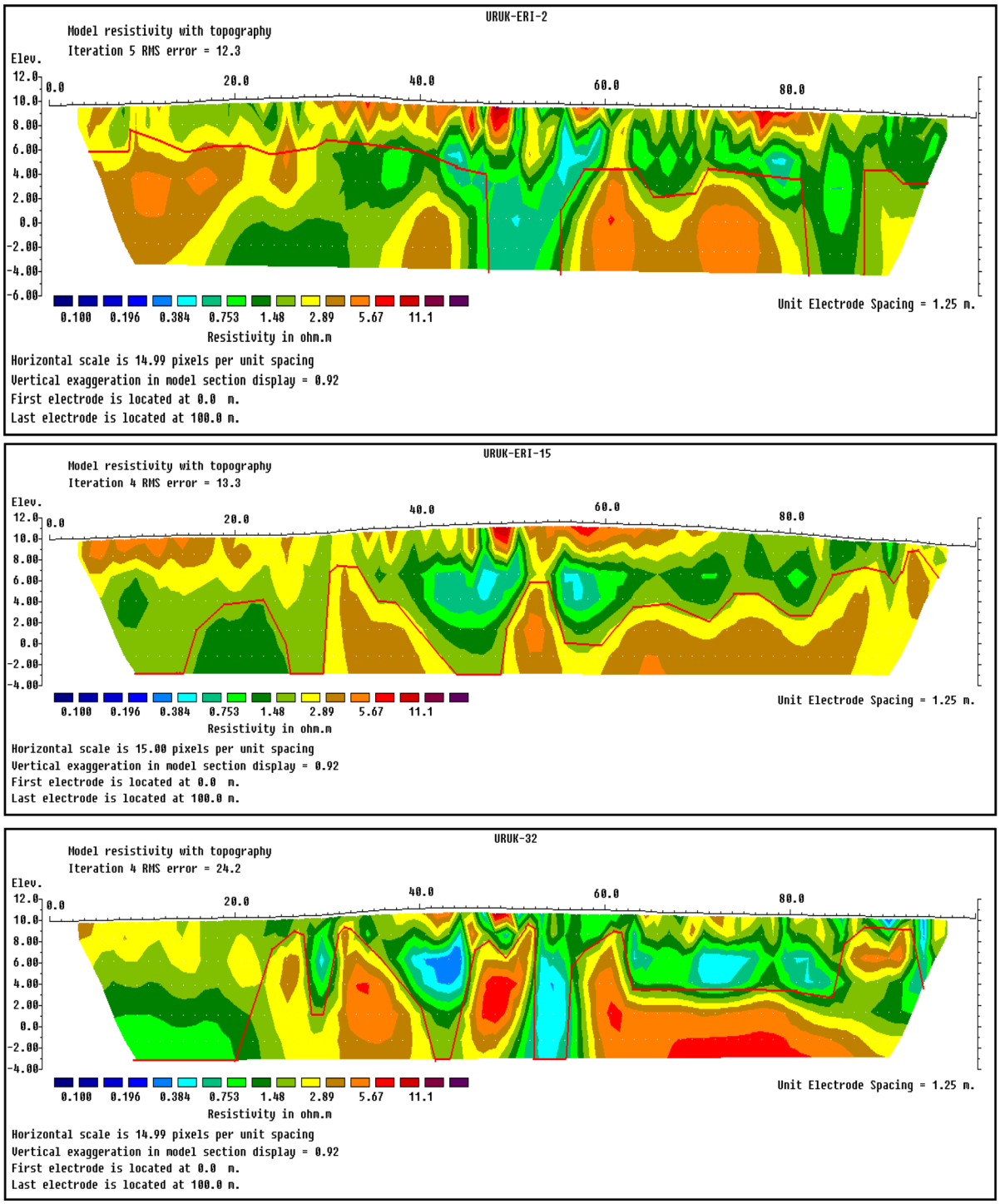

Figure 13
Interpreted 2D inverse model of profiles 12, 15 and 32 as some examples from the area under study

mainly of clay. The highest resistive areas nearby the surface are caused by the dried upper layers. In this zone, some anomalies caused by boulders with resistivity equal to 5.67 Ohm m can be seen at depth 0.5 m from the surface. The second zone shows a prominent lower resistive (0.753 Ohm m) zone below the first one. This is probably caused by the moisture in this region that reduces the resistivity. Thickness of this layer differs from other parts of the site. In addition, some anomalous archaeological materials (5.67 Ohm m) related to core boulders, air cavities or graves presented at this zone can clearly be observed. Underneath this intermediate zone is a more resistive zone which indicates more intact zone of archaeological structures down to the bottom of the image. The images indicate that an archaeological structure extended vertically through the images is most probably related to the buried remains and ruins of old buildings and walls that have resistivity values which are either low (0.384 Ohm m) or resistive (5.67–11 Ohm m) at depth ranging from 6 m to 13.5 m related to the archaeological wall.

3.3. Comparison Between GPR and ERT

Figures 14 and 15 show examples of both GPR and ERT results at the Babylonian houses district. The reflections existed within the radargrams are described in terms of reflection continuity, shape, amplitude, internal reflection configuration and external form (pattern of reflections). It seems that the GPR profile has a maximum depth of investigation of 1–6 m depending on the subsoil case. The GPR images demonstrate deeper anomalies characterized by continuous reflections with different widths. These deeper reflections correspond to a zone on the 2D-resistivity models with the higher resistive archaeological walls of the third zone extending vertically through the images. The GPR images show reflections of attributes which are presented at the

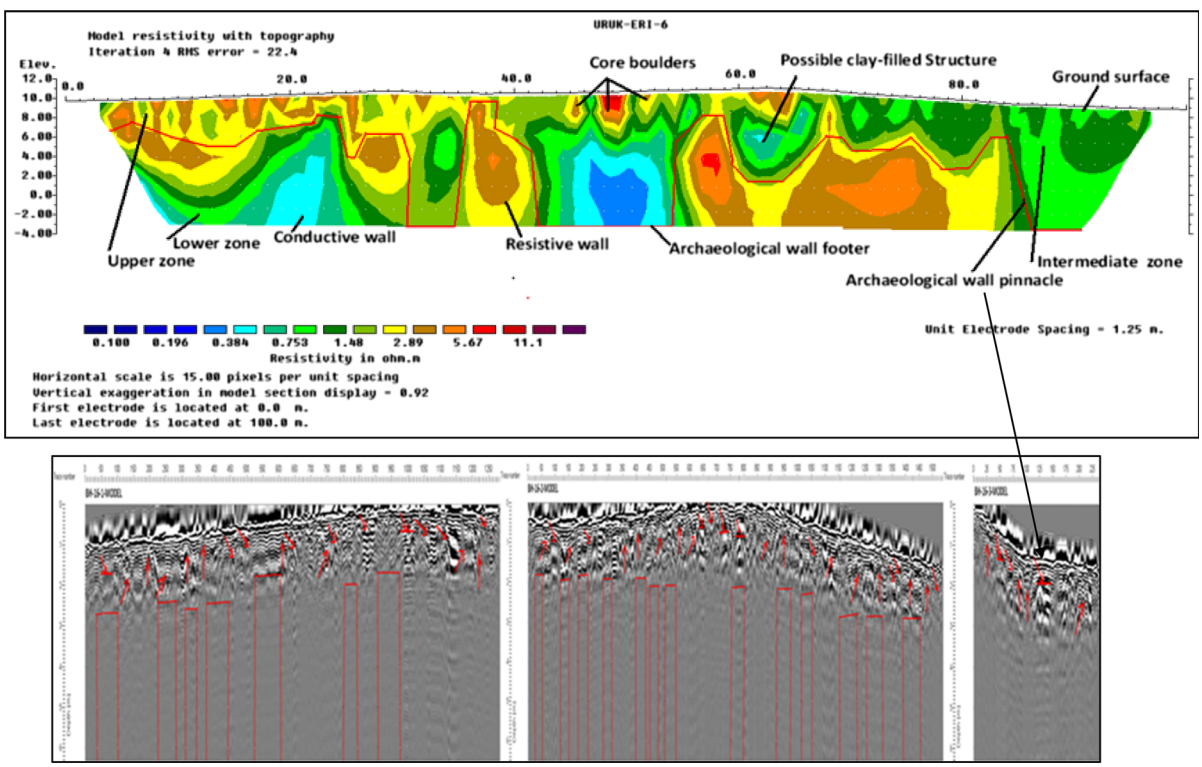

Figure 14
Interpreted inverse model of ERT (profile-6) and its corresponding GPR segment profiles within the area

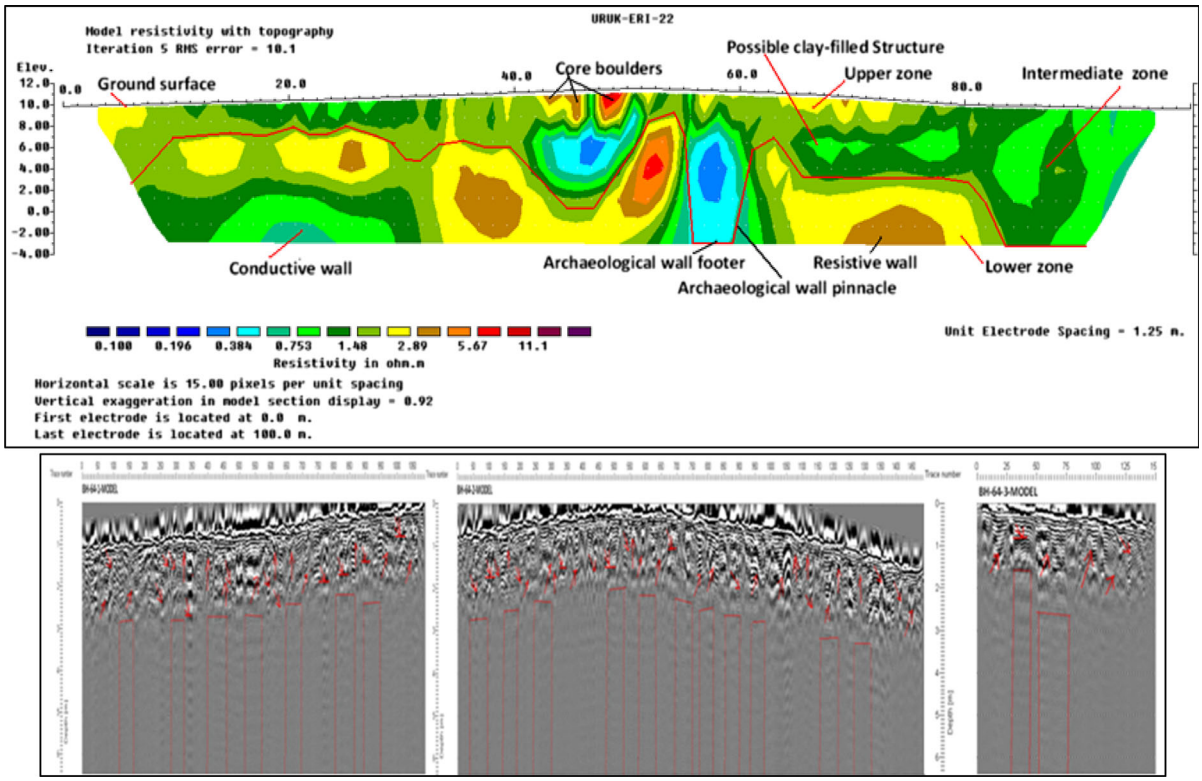

Figure 15
Interpreted inverse model of ERT (profile-22) and its corresponding GPR segment profiles within the area

shallower depth and characteristic for the upper part of the district and can often be found throughout the area and represent the top part of the Babylonian houses. However, the ERT sections also show the upper zone near the surface of the earth with a highly resistivity value. There is intermediate lower resistive layer with thickness differing from parts to others within the study site. Also, the GPR and ERT anomalies are characterized by the existence of dense and buried items, buried trenches and pits or object.

The GPR profiles have maximum depth of investigation of 6 m and ERT profiles have maximum depth of investigation of 13.5 m. These results establish whether the information from GPR and ERT is complementary in delineating the subsurface. According to the previous results, it is clear that the two methods are integrated and used for completing the description of the area understudy.

A contour map (Fig. 16) and 3D-view (Fig. 17) of the distribution of the archaeological anomalies at the study area were plotted using data of the ERT transects (from the 2D-resistivity line 1–32) and GPR transects (from the GPR line 1 to GPR line 90) with the assistance of Surfer and GIS programs, respectively. These data represent the anomalies at the study area; therefore, high anomaly means high elevation of the old wall present at the certain location and vice versa. The wall footer indicates the absence of the archaeological wall at this location. The values of the elevations of the walls are taken as guide for the archaeological anomalies. These 2D and 3D maps of the archaeological foundations of Uruk site show that the archaeological anomalies are concentrated mainly at the NE part of the district. Additionally, high values of anomalies are concentrated along this direction. In this part of the district, the walls are higher than that at the SW, SE and NW parts ranging mainly from 6 to 8 m and exceed 10 m in some locations at the NE area. At the remaining parts trending SW, SE and NW, the walls are lower in

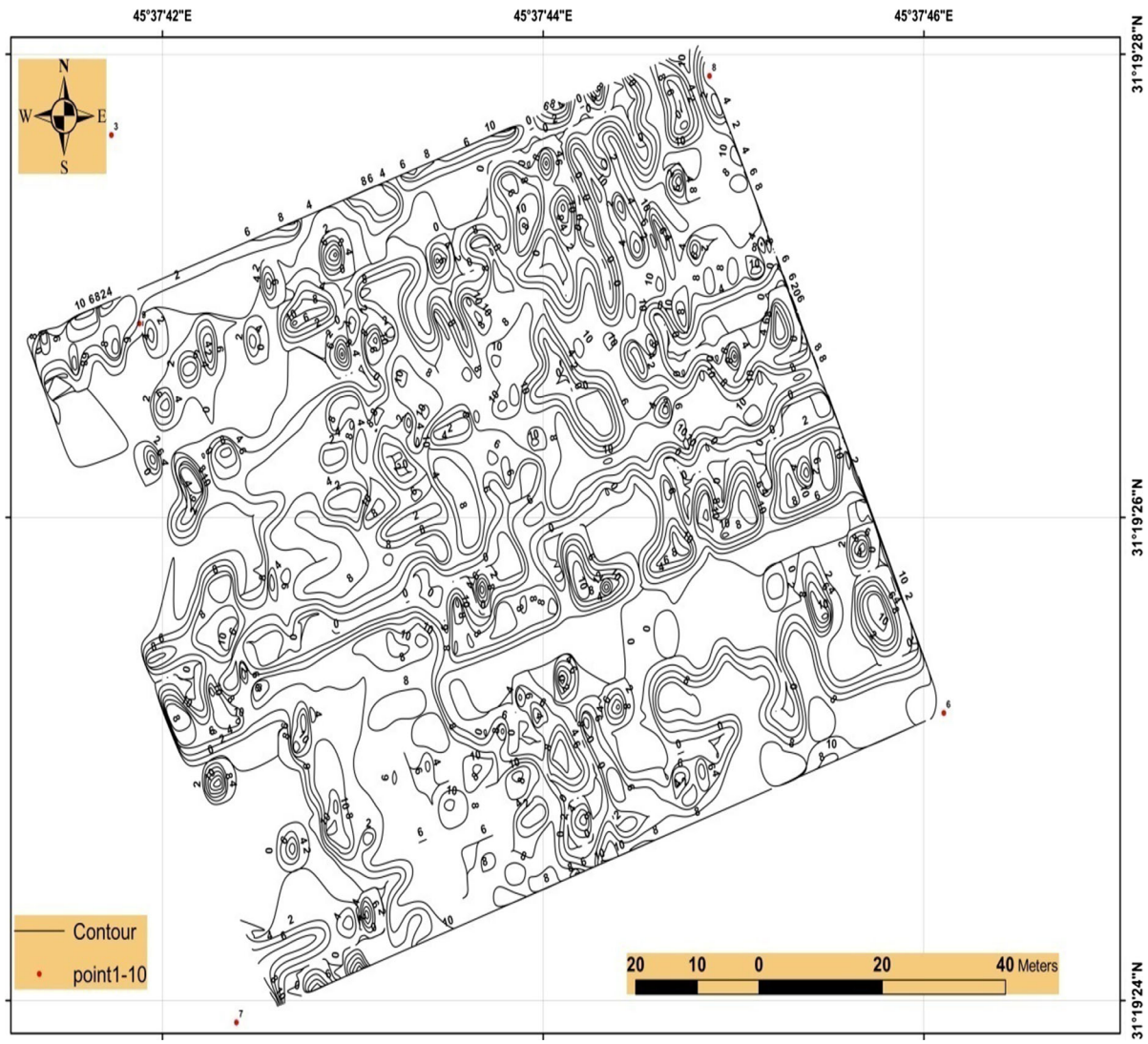

Figure 16
Map shows anomalies of the archaeological foundations of Uruk site from GPR and 2D-imaging data

heights ranging mainly between 4 and 6 m. In some places (especially at the west part) of district, the height of the wall reaches the wall foot.

4. Conclusions

According to the GPR and ERT profiles' interpretation of the study area, it seems that the acquired GPR radargrams show large and continuous signal attributes with different widths. In radargrams, at the shallower depth, GPR attributes strongly represent the upper part of Babylonian Houses throughout the study area. Besides, some objects such as buried items, buried trenches and pits were mainly concentrated near the surface.

ERT dipole–dipole array results show the presence of several anomalies at different depths mostly having low resistivities. Thus, it is clear that the first upper zone can often be found throughout the whole area and it may represent the top zone of the Babylonian houses that consists of dry clay and sandy soil including some broken bricks and slag mixed with core boulders distributed here and there at the

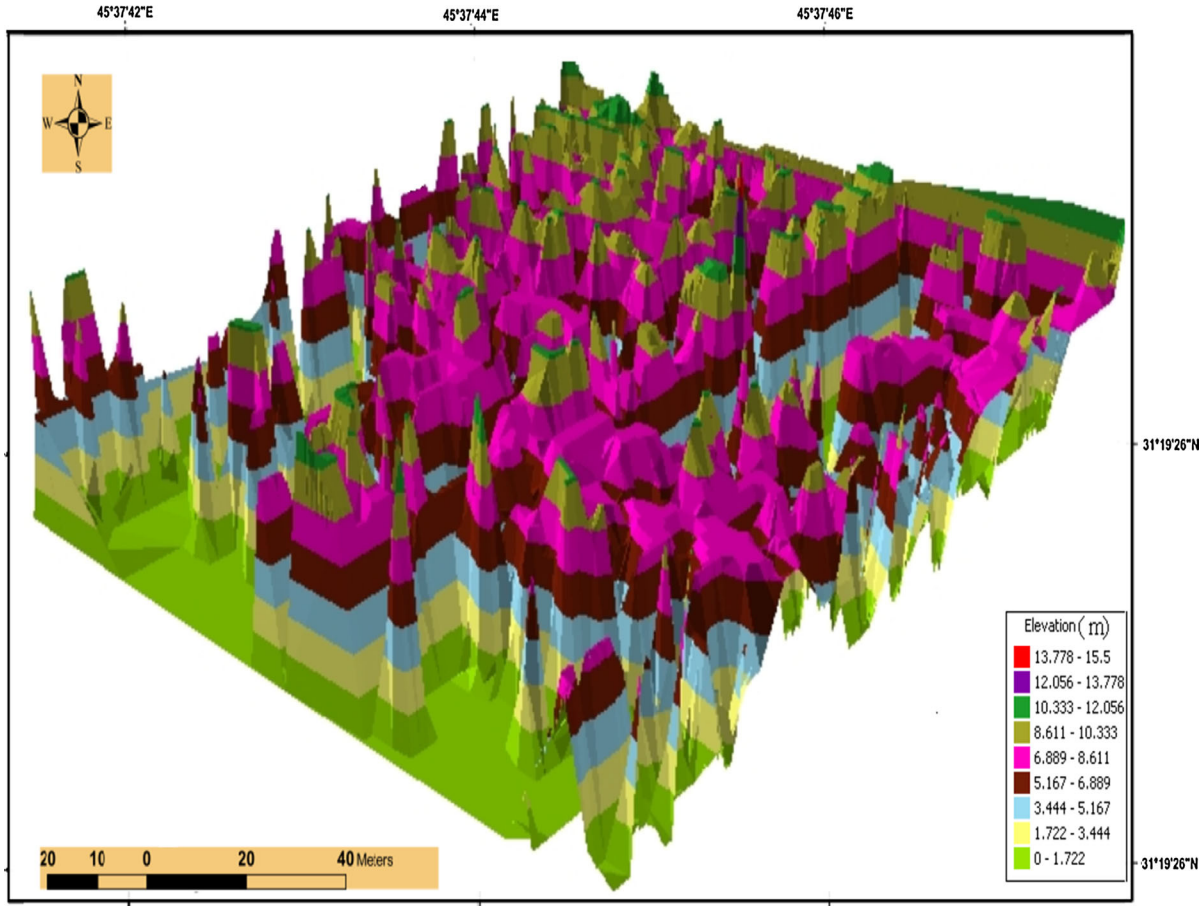

Figure 17
3D view of the archaeological foundations of Babylonian houses data

surface. The second zone clarifies a prominent lower resistivity zone. It is probably presented by the moisture content that reduces the resistivity. The thickness of this zone is not equal at all parts of the site. Finally, the third deeper zone typically represents the archaeological walls. Most of the distinct anomalies perhaps referred to the buried clay brick walls.

The constructed map of the archaeological anomalies distribution and 3D view of the foundations at the study area using GPR and ERT methods clearly demonstrate the characteristics of the Babylonian remains. A contour map and 3D view of Uruk show that the archaeological anomalies are concentrated at the NE part of the area understudy having highly walls height that ranging between 6–8 m and up to more than 10 m in some places. At the other directions, there are fewer walls with lower heights of 4–6 m and seem in some places closer to the wall foot.

Acknowledgments

The authors are highly grateful to Dr. Firas H. Al-Menshed and Dr. Ahmed S. Al-Zubedi for their sincere assistance in the field works. Thanks also extend to Dr. Ali Z. Al-Khashan for reading the manuscript of the present research.

REFERENCES

AIZEBEOKHAI, A. P., (2010), *2D and 3D geoelectrical resistivity imaging, Theory and field design*, Scientific Research and Essays Vol. *5*, 14p.

AL-HASHIMI, H., (1974), Stratigraphy and palaeontology of the subsurface rocks of Samawa Area, SOM, Iraq.

BAKER, H. D., (2002), The Urban landscape in first millennium BC Babylonia, University of Vienna.

BARKER, R.D., (1992), *A simple algorithm for electrical imaging of the subsurface*, First Break, Vol. *10*, No. 2, 10p.

BEAULIEU, P., (2003), The Pantheon of Uruk during the Neo-Babylonian period, 424p.

BUDAY, T., (1980), Regional geology of Iraq, Stratigraphy and Palaeogeography, GEOSURV, Baghdad, Iraq, Vol. 1, 445p.

DAHLIN, T. and ZHOU, B., (2004), *A numerical comparison of 2D resistivity imaging with ten electrode arrays*, Geophysical Prospecting, Vol. *52*, 20 p.

FASSBINDER, J. and BECKER, H., (2001), "Uruk-City of Gilgamesh (Iraq) First tests in 2001 for magnetic prospecting", dans Becker, H., Fassbinder, J. W.E, Magnetic prospecting in Archaeological Sites, Vol. VI, 5p.

FASSBINDER, J., BECKER, H. and VAN ESS, M. (2003), Prospections magnetiques a Uruk (Warka): La cite du roi Gilgamesh (Irak).

HRITZ, C., (2012), History and Archaeology in Southern Mesopotamia, Department of Anthropology, Pennsylvania State University Basrah.

LOKE, M.H. and DAHLIN, T., (2002), *A comparison of Gauss-Newton and quasi-Newton methods in resistivity imaging inversion*. Journal of applied geophysics, vol. *49*, 19 p.

LOKE, M.H., (2004), Tutorial: 2D and 3D electrical imaging surveys, 127p.

LOKE, M.H., (2010), Tutorial: 2D and 3D electrical imaging surveys, 154p.

OSWIN, J., (2009), A Field guide to geophysics in archaeology, Praxis Publishing, No 2009925774, Chic Ester, UK, 243p.

POLLOCK, S., POPE, M. and COURSE, Y., (1996), *Household production at the Uruk Mound, Abu Salabikh, Iraq*, American Journal of Archaeology, Vol. *100*, No. 4, 16p.

(Received June 26, 2014, revised July 29, 2015, accepted August 1, 2015)